ACS chemical biology

Articles

pubs.acs.org/acschemicalbiology

Selective Aurora Kinase Inhibitors Identified Using a Taxol-Induced Checkpoint Sensitivity Screen

Nicholas Kwiatkowski,[†,‡,#] Xianming Deng,[†,‡,#] Jinhua Wang,[†,‡] Li Tan,[†,‡] Fabrizio Villa,[∥] Stefano Santaguida,[∥,¶] Hsiao-Chun Huang,[§] Tim Mitchison,[§] Andrea Musacchio,[∥,⊥] and Nathanael Gray[†,‡,*]

[†]Department of Cancer Biology, Dana Farber Cancer Institute, [‡]Department of Biological Chemistry and Molecular Pharmacology, and [§]Department of Systems Biology, Harvard Medical School, Boston, Massachusetts 02115, United States

[∥]Department of Experimental Oncology, European Institute of Oncology, Via Adamello 16, 20139 Milan, Italy

[⊥]Max Planck Institute of Molecular Physiology, Otto-Hahn-Strasse 11, 44227 Dortmund, Germany

Supporting Information

ABSTRACT: The members of the Aurora kinase family play critical roles in the regulation of the cell cycle and mitotic spindle assembly and have been intensively investigated as potential targets for a new class of anticancer drugs. We describe a new highly potent and selective class of Aurora kinase inhibitors discovered using a phenotypic cellular screen. Optimized inhibitors display many of the hallmarks of Aurora inhibition including endoreduplication, polyploidy, and loss of cell viability in cancer cells. Structure−activity relationships with respect to kinome-wide selectivity and guided by an Aurora B co-crystal structure resulted in the identification of key selectivity determinants and discovery of a subseries with selectivity toward Aurora A. A direct comparison of biochemical and cellular profiles with respect to published Aurora inhibitors including VX-680, AZD1152, MLN8054, and a pyrimidine-based compound from Genentech demonstrates that compounds **1** and **3** will become valuable additional pharmacological probes of Aurora-dependent functions.

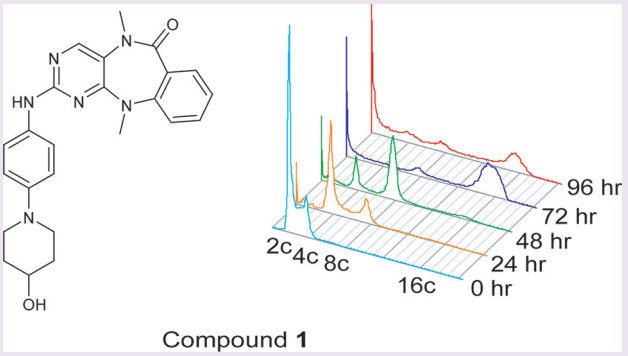

The inhibition of critical regulatory mitotic kinases using ATP-competitive small molecules is an active area of research in the quest for a new class of anticancer therapeutics. Numerous compounds targeting key cell cycle kinases including Cyclin-dependent kinases (Cdk), Aurora (Aur), Polo-like kinases (Plk), and the kinesin-5 molecular motor have been advanced into the clinical testing. The clinical rationale for targeting mitosis to treat cancer is provided by Taxol, a highly successful anticancer agent that arrests cell division by stabilizing microtubule polymers and thereby disrupting the cellular machinery required for mitotic spindle assembly. Unfortunately, to date most of the small molecules targeting cell cycle kinases have displayed limited clinical efficacy and have suffered from dose-limiting bone marrow toxicity. We hypothesized that there might exist small molecule kinase inhibitors that synergize with Taxol, augmenting the anti-proliferative and apoptotic response.

Previous reports have demonstrated that the cell death response to Taxol treatment is dependent upon the ability of cells to maintain a mitotic arrest.[1−3] This phenomenon has been attributed, in part, to post-translational modification and inactivation of anti-apoptotic proteins during mitosis allowing for engagement of a productive apoptotic response.[4−6] This post-translational modification is lost when cells exit mitosis, leading to stabilization of anti-apoptotic proteins and concomitant decrease in Taxol-mediated cell death. Therefore, we hypothesized that the identification of a small molecule that maintained a mitotic arrest independent of the spindle assembly checkpoint (SAC) status could potentiate the apoptotic response to Taxol. Conversely, a small molecule that inhibits the SAC would be expected to weaken the apoptotic response to Taxol. We performed a medium-throughput proliferation assay of approximately 1000 known and novel small molecule kinase inhibitors alone and in combination with Taxol to find compounds that could agonize or antagonize the anti-proliferative effects of Taxol. One class of compounds that emerged as antagonists of Taxol-induced growth inhibition from this screening effort was a series of pyrimido benzodiazepines exemplified by compounds **1** and **3**. A candidate-based approach combined with extensive chemical proteomic and kinase binding panel-based profiling efforts

Received: August 18, 2011
Accepted: October 12, 2011
Published: October 12, 2011

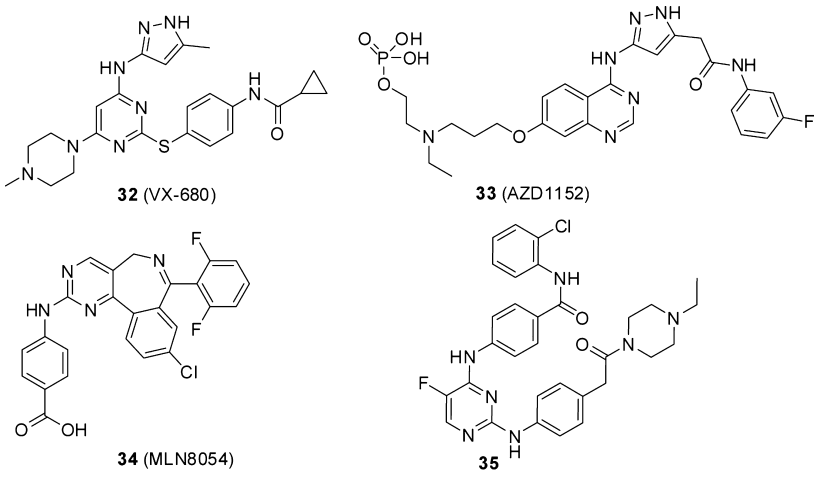

Figure 1. Structures of known Aurora inhibitors.

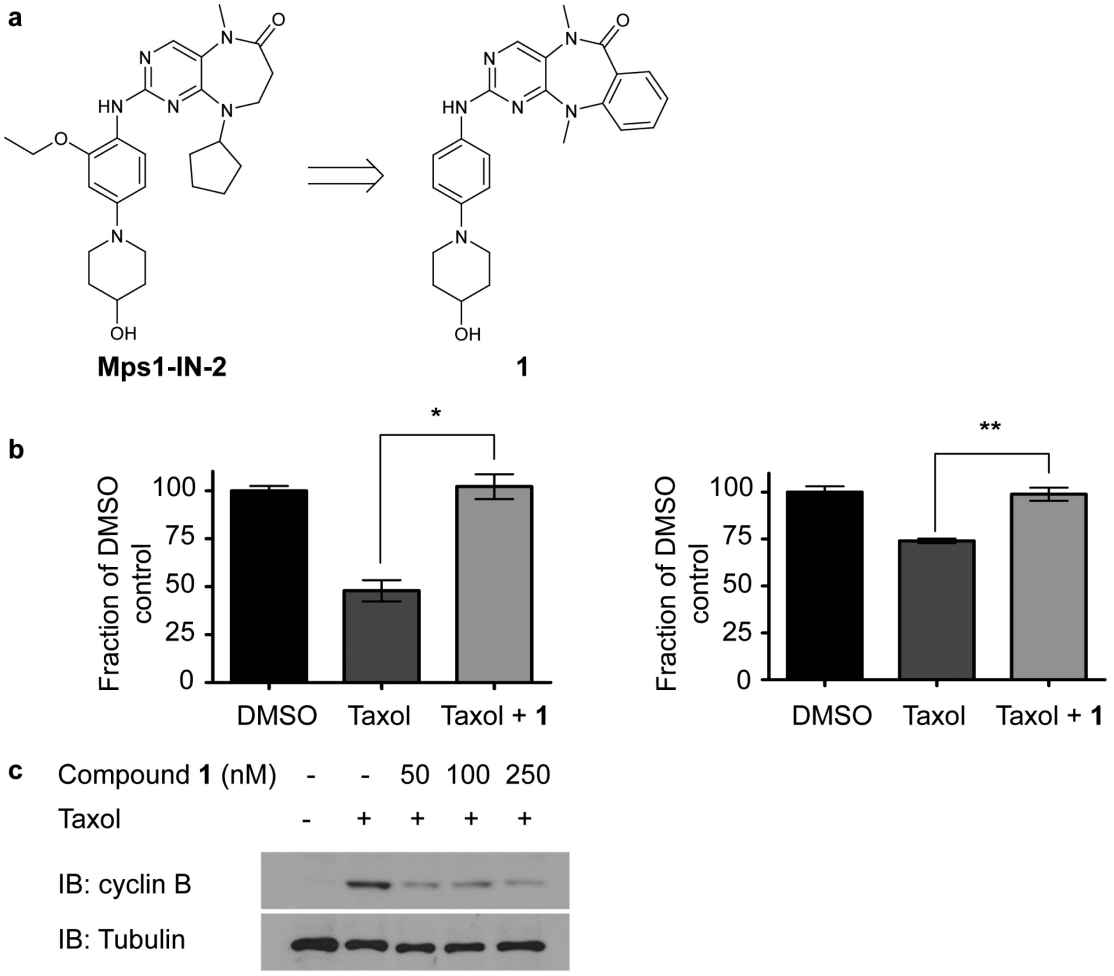

Figure 2. Taxol sensitivity screen identifies new SAC inhibitor series. (a) Chemical structures of Mps1-IN-2[41] and compound **1**. (b) Results of Taxol sensitivity screen for compound **1**. Hela (left panel) and MCF7 (right panel) cells were treated with DMSO, Taxol (100 nM), or Taxol with **1** (50 nM) for 48 h. **p*-value = 3.15×10^{-3}, ***p*-value = 2.51×10^{-3}. (c) Mitotic escape assay in the presence of **1**. Mitotic exit was determined by the stability of cyclin B protein levels, a mitotic marker.

established that these compounds are potent Aurora A/B kinase inhibitors.

Aurora A and B share significant sequence similarity, particularly within their kinase domains; however, each kinase exhibits unique precise temporal and spatial control by dynamic association with accessory proteins.[7−19] These interactions allow Aurora A and B to independently regulate many important mitotic processes. Aurora A regulates the separation of centrosomes in S phase/early G2[20−22] and contributes to bipolar spindle formation in mitosis by regulating microtubule (MT) nucleation, bundling, and stabilization.[23−25] Aurora B facilitates proper bipolar end-on MT-kinetochore attach-

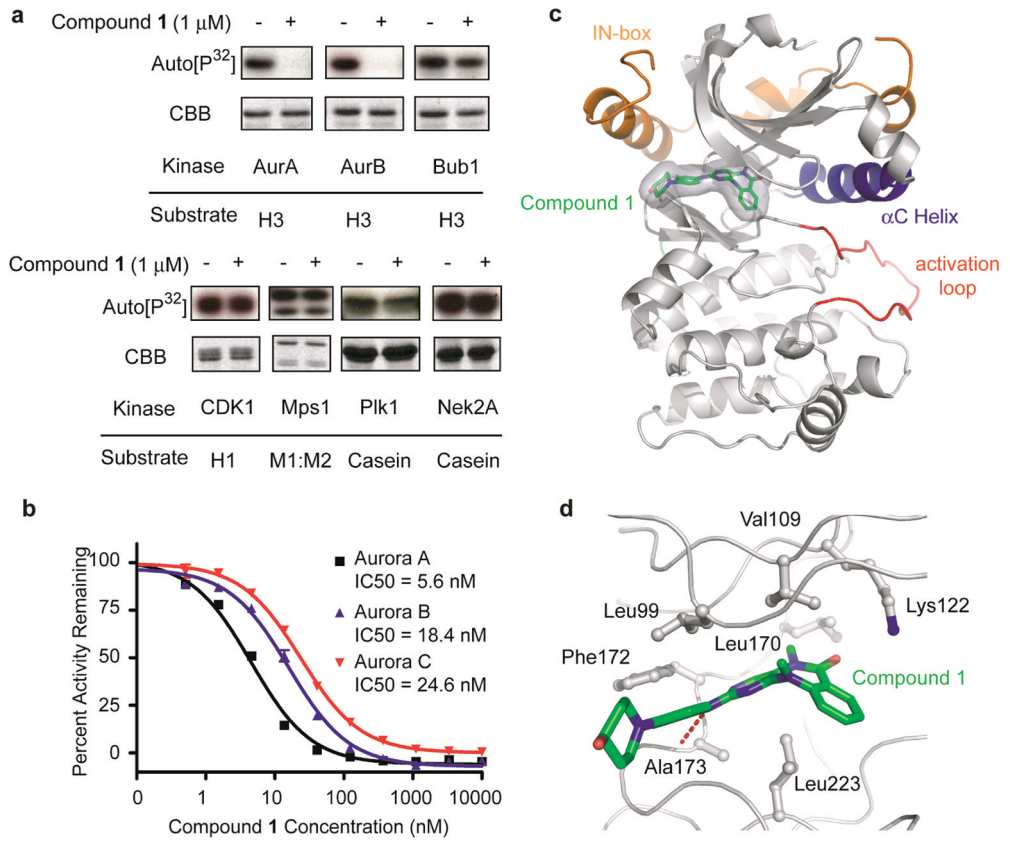

Figure 3. Compound **1** inhibits Aurora kinases. (a) Effect of **1** treatment on the kinase activities of a panel of mitotic kinases. *In vitro* kinase assays were performed to determine the extent of inhibition by **1** on the kinases in the panel. (b) *In vitro* kinase assays of Aurora A, B, and C using Z-LYTE technology (Invitrogen) and ATP at K_m apparent for each kinase. Each concentration point was performed in duplicate. (c) Interaction of compound **1** with the Aurora B ATP-binding pocket. Aurora B^{60-361} (gray) contains the kinase domain of Aurora B and is represented as a cartoon. Some features, including the C-terminal extension (green), the activation loop (red), and the αC helix (blue), are highlighted. $INCENP^{790-847}$ (IN-box, orange) crowns the small lobe of Aurora B, stabilizing an active conformation of the kinase.[21] Compound **1**, shown as sticks and surrounded by a semitransparent surface, occupies the ATP-binding pocket at the interface between the small and large lobes. (d) Ball-and-stick representation of the interaction of compound **1** with selected residues of Aurora B. Oxygen and nitrogen atoms are shown in red and blue, respectively. Carbon atoms in compound **1** and in Aurora B are green and gray, respectively. Hydrogen bonds are shown as dashed lines (red). Auto[^{32}P], autoradiography [^{32}P]; CBB, Coomassie Brilliant Blue. Images were created with pymol (PyMOL Molecular Graphics System, www.pymol.org).

ment,[26−28] participates in SAC signaling,[29−31] and mediates chromosome condensation and cohesion.[32] Aurora B relocalizes to the central spindle during late anaphase and to the midbody during telophase, thereby facilitating cytokinesis.[33] Chemical perturbation of Aurora kinases has proven invaluable in parsing the temporal and spatial functions of each isoform and assessing the therapeutic potential in inhibiting kinase activity in the context of cancer.

Detailed biochemical and cellular mechanism of action studies demonstrated that these inhibitors potently inhibited the Aurora kinases at low nanomolar concentration in cells. Compound treatment faithfully recapitulated phenotypes associated with RNAi and chemical inhibition of Aurora A[20−22,32] and B[16,26−28,30,33] kinases including monopolar spindle formation, cytokinesis failure, and polyploidy. Additionally, compound **1** efficiently disables the SAC, which is consistent with the known requirement for a Taxol-induced arrest requiring a functional checkpoint. We co-crystallized **1** with the *Xenopus laevis* Aurora B/INCENP complex and determined the structure at 1.85 Å resolution. We used this structure in conjunction with kinome-wide selectivity profiling to guide chemical modifications that allowed the identification of key selectivity determinants and the generation of Aurora A-selective agents. We compared the anti-proliferative effects of these new Aurora kinase inhibitors to 4 literature compounds: VX680 (compound **32**), a pan-Aurora inhibitor; AZD1152 (compound **33**), an Aurora B selective agent, and two Aurora A-selective compounds, MLN8054 (compound **34**) and a pyrimidine-based compound from Genentech (compound **35**) (Figure 1).[34−37] Consistent with previous studies, the comparison of these compounds to existing Aurora inhibitors demonstrates that much of their anti-proliferative activity is derived from inhibition of Aurora B.[38]

RESULTS AND DISCUSSION

Phenotypic Screen Identifies SAC Inhibitor. In order to identify compounds that could modulate the spindle assembly checkpoint, we performed a proliferation screen for compounds that could synergize or antagonize with Taxol. We screened a diverse library (~1000 compounds) of heterocyclic ATP-site directed kinase scaffolds in dose−response format to identify new small molecule modulators of Taxol-induced mitotic arrest and cell death. We conducted the screen in Hela and MCF7 cell lines that are sensitive and resistant to Taxol-induced cell death, respectively.[3] Compounds eliciting a differential effect in combination with Taxol when compared to Taxol alone were

dx.doi.org/10.1021/cb200305u | ACS Chem. Biol. 2012, 7, 185−196

Table 1. Enzymatic and Anti-proliferative Activities for Benzo[*e*]pyrimido[5,4-*b*][1,4]diazepin-6(11*H*)-ones 1−18

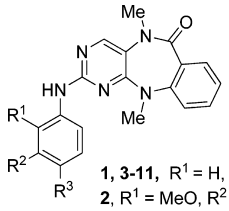

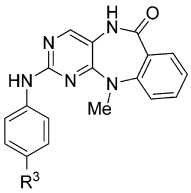

18

Compd ID	Structure	Enzyme IC_{50} (nM)[a]		Cell EC_{50} (nM)[b]		
		Aur A	Aur B	HCT 116	HT29	HeLa
1	R^3 = 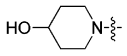	5.6	18.4	9.5	55	16.7
2	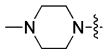	1210	3440	-[c]	-	-
3	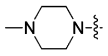	7.2	25.9	19	68	10.9
4	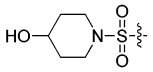	8.8	28.6	-	-	-
5	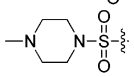	16.8	45.1	-	-	-
6		3.4	8.4	75.1	390	80.1
7	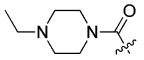	5.9	15.2	56.7	195	16.9
8	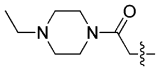	6.1	18.7	87	621	61.7
9	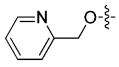	18.4	39.3	-	-	-
10	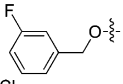	323	512	-	-	-
11	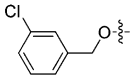	83.9	352	-	-	-
12	R^2,R^3 = CF_3, 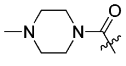	9.0	84.8	475	796	560
13	CF_3, 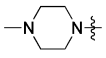	86.8	774	-	-	-
14	Cl, 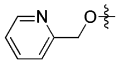	53.2	417	-	-	-
15	R^2 = 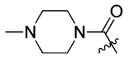	14.9	36.7	-	-	-
16	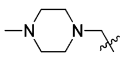	10.7	19.8	-	-	-
17	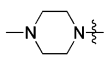	11.9	55.8	-	-	-
18	R^3 = 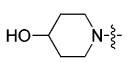	98.5	216	-	-	-

[a]The required concentration to inhibit 50% of enzyme activity. [b]The required concentration for inhibiting cell growth at 50%. [c]"−" means not tested.

then studied for their effect on cell cycle progression. We identified a broad class of pyrimidodiazepinone compounds that represent a privileged ATP-site directed scaffold that has been successfully elaborated to generate selective inhibitors of Erk5, LRRK2, and Mps1.[39−41] For example, the benzo[*e*]-pyrimido[5,4-*b*][1,4]diazepin-6(11*H*)-ones, represented by compound **1** (Figure 2a), emerged as a particular promising hit compound. When cells were co-treated with Taxol (100

dx.doi.org/10.1021/cb200305u|*ACS Chem. Biol.* 2012, 7, 185−196

Table 2. Enzymatic and Anti-proliferative Activities for Benzo[*e*]pyrimido[5,4-*b*][1,4]diazepin-6(11*H*)-ones 19−31

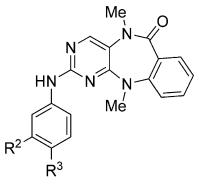

19-22

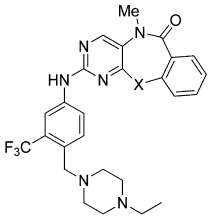

23-27

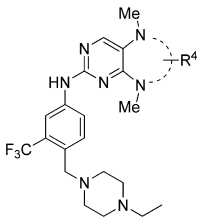

28-31

Compd ID	Structure	Enzyme IC_{50} (nM)[a]		Cell EC_{50} (nM)[b]		
		Aur A	Aur B	HCT 116	HT29	HeLa
12	R^2,R^3 = CF_3, 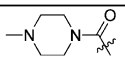	9.0	84.8	-[c]	-	-
19	CF_3, 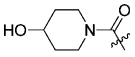	5.1	43.7	591	1315	883
20	Cl, 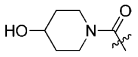	3.2	14.3	-	-	-
21	CH_3, 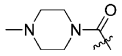	3.7	14.5	26.9	290	28
22	MeO, 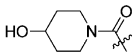	2.6	24.2	207	843	378
23	X = 	16.8	194	553	951	1300
24		81.7	782	-	-	-
25		102	971	-	-	-
26	O	457	3040	-	-	-
27	S	535	3820	7260	3797	>10000
28	R^4 = 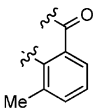	11.6	132	238	911	>10000
29	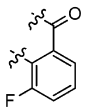	13.4	487	449	1577	792
30	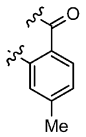	146	230	-	-	-
31	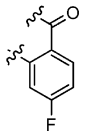	298	586	-	-	-

[a]The required concentration to inhibit 50% of enzyme activity. [b]The required concentration for inhibiting cell growth at 50%. [c]"−" means not tested.

nM) and **1** (50 nM), there was a significant reduction in cell survival compared to Taxol as a single agent over a 48 h time period (Figure 2b). Consistent with the notion that abrogation of mitotic arrest mitigates cell death caused by microtubule stabilizers, compound **1** treatment resulted in a premature exit from a Taxol-induced mitotic arrest (Figure 2c). These results suggested that **1** was capable of functioning as an inhibitor of the spindle assembly checkpoint.

Compound 1 Potently Inhibits Aurora Kinases. In order to identify the molecular target(s) of **1**, we pursued a candidate-based approach and investigated the ability of **1** to inhibit the enzymatic activity of mitotic kinases known to affect SAC-mediated arrest such as Aurora A, Aurora B, Bub1,

dx.doi.org/10.1021/cb200305u|*ACS Chem. Biol.* 2012, 7, 185−196

CDK1/cycB, Plk1, Mps1, and Nek2A (Figure 3a). Compound **1** potently and selectively inhibited the enzymatic Aurora A, B, and C kinases with IC_{50}'s of 5.6, 18.4, and 24.6 nM, respectively (Figure 3b). The selectivity of these inhibitors was surprising considering the structural similarity of **1** to previously reported kinase inhibitors.[39−42] For example, the slight modification from a two-ring system, exemplified by Mps1-IN-2 and BI2536, to a three-ring system, exemplified by **1**, was sufficient to abrogate the ability of **1** to inhibit Mps1 and Plk1 activity. The structural basis for this result will be discussed in the following section.

Crystal Structure of Aurora B: INCENP in Complex with Compound 1. We determined the crystal structure of the Aurora B:INCENP complex from *Xenopus laevis*[21] in complex with compound **1**. The crystals contain a tight complex of residues 60−361 of Aurora B (Aurora B^{60-361}) and residues 790−847 of INCENP ($INCENP^{790-847}$), the so-called IN-box (Figure 3c). Crystals of the Aurora B:INCENP complex with compound **1** diffracted X-rays to a resolution of 1.85 Å (Supplementary Table S1). Electron density "difference" maps with phases calculated from the model of the Aurora B^{60-361}:$INCENP^{790-847}$ complex revealed additional density in the Aurora B ATP-binding pocket (Figure 3c). The density could be fitted unequivocally with an atomic model of compound **1**. As expected, the inhibitor bound to the ATP binding pocket of Aurora B, hydrogen-bonded to the carbonyl of Ala173 within the hinge backbone. No significant structural rearrangements of the kinase backbone are observed in the presence of the compound (Supplementary Figure S1). Binding is stabilized by a number of hydrophobic interactions involving Leu170 (the gatekeeper residue), Phe172, Leu223, and the P-loop residues Leu99 and Val107 (Figure 3d).

To rationalize the observed selectivity of **1** for Aurora-family kinases, we superimposed the models of Aurora A, Mps1, and Plk1 onto the Aurora:INCENP:compound **1** structure. We then assessed if **1** could at least in principle be accommodated without major steric clashes in these additional active sites (Supplementary Figure S2). As expected on the basis of the high sequence conservation relating Aurora A and Aurora B, compound **1** could be nicely modeled in the Aurora A catalytic cleft, probably accounting for the 5.6 nM IC_{50} (Supplementary Figure S2a,b). On the other hand, a predicted steric clash between large hydrophobic residues in the active sites of Mps1 and Plk1 (Ile663 and Phe169, respectively) and the additional anthranilic ring of compound **1** is probably the cause of the poor inhibitory activity of compound **1** against these kinases (Supplementary Figure S2). Interestingly, a *cis* peptide bond between Ile663 and Asp664 in the Mps1 active site causes a potential clash against the third ring of the pyrimido benzodiazepine moiety (Supplementary Figure S2).

Summary of Structure−Activity Relationships. Having assessed the intracellular activity and *in vitro* selectivity of **1**, we sought to evaluate the potential of this scaffold to generate selective Aurora A or Aurora B agents. For these structure−activity relationship (SAR) studies, we desired to efficiently modify the 2-amino and fused anthranilic acid moieties of the core benzo[*e*]pyrimido[5,4-*b*][1,4]diazepin-6(11*H*)-one scaffold. To do so, we developed a concise four-step synthetic route to complete the synthesis of a comprehensive analogue library of our initial screening hit, compound **1**.[40] Details of the synthetic methods and compound characterization are described in the Supporting Information.

Approximately 30 benzo[*e*]pyrimido[5,4-*b*][1,4]diazepin-6-(11*H*)-one analogues were evaluated for their ability to inhibit Aurora A and B kinase activity (IC_{50} data, Tables 1 and 2; SAR data, Figure 4). Comparison with our previously developed

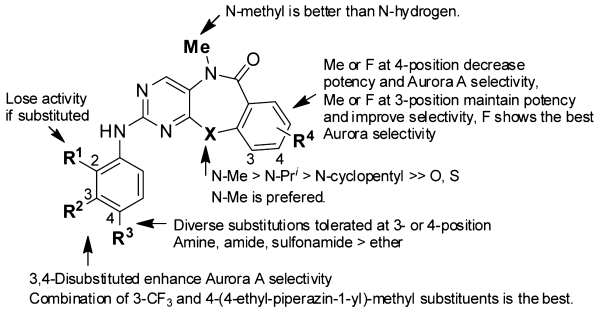

Figure 4. Summary of SAR for benzo[*e*]pyrimido[5,4-*b*][1,4]diazepin-6(11*H*)-one Aurora inhibitors.

ERK5[40] and LRRK2[39] inhibitors revealed that substitution of the *ortho*-position of the 2-anilino moiety of **1** is not tolerated for potent Aurora inhibition (compound **2** *vs* **3**), likely due to steric clash with Phe172 (Figure 3d). We first explored the 2-amino moiety of this scaffold by replacing the aniline substituent of **1** with various 3-substituted, 4-substituted, and 3,4-disubstituted anilines (Table 1). These modifications all yielded compounds possessing similar activity against Aurora A and B. These results indicated that diverse substitutions at 3- or 4-position of 2-aniline moiety were well tolerated but did not impart significant selectivity between Aurora kinases. Interestingly, when 3,4-disubstituted anilines were introduced, these analogues (**12**−**14**) showed much better *in vitro* activity against Aurora A compared with that against Aurora B (compounds **12** *vs* **7**, **13** *vs* **3**, and **14** *vs* **9**). This result suggested that additional substituents at the 3-position will affect the selectivity of Aurora A *vs* B. Compound **18** containing an unsubstituted lactam amide exhibited a 10-fold decrease in activities for both Aurora kinases, which indicated the methyl substitution of the lactam is preferred.

We next investigated the effects of additional substituents at the 3-position of aniline with respect to Aurora A *vs* B selectivity (**19**−**23**, Table 2). Compound **23** having the combination of 3-trifluoromethyl and 4-(4-ethyl-piperazin-1-yl)-methyl substituents gives the best *in vitro* selectivity with an IC_{50} ratio of 12. We then fixed 3-trifluoromethyl-4-(4-ethyl-piperazin-1-yl)-methyl aniline at the 2-position of benzo[*e*]-pyrimido[5,4-*b*][1,4]diazepin-6(11*H*)-one and studied the effects of modification to the N-substituent (X) of the anthranilic acid and to the aryl ring (R^3) (**24**−**31**, Table 2). Modification of the N-substituent (X) from methyl, to isopropyl, to cyclopentyl, exemplified by **23**, **24**, and **25**, respectively, led to gradual decreases in enzyme activity and selectivity. Linkages using oxy (**26**) or sulfur (**27**) resulted in a dramatic loss of activity. These results suggest that modifications to the N-substituent (X) are not well tolerated because the linkage groups are the determinant of the dihedral angle of the seven-membered ring. There appears to be a great effect of substituent position for selectivity as the 3-methyl, 4-methyl, 3-fluoro, and 4-fluoro analogues (**28** *vs* **30**, **29** *vs* **31**) exhibited marked difference in selectivity of Aurora A *vs* B. Among them, compound **29** represented the best *in vitro* selectivity (36-fold) and activity of 13.4 nM for Aurora A. Facing the 3-position of the aniline group in Aurora A and

dx.doi.org/10.1021/cb200305u | *ACS Chem. Biol.* 2012, 7, 185−196

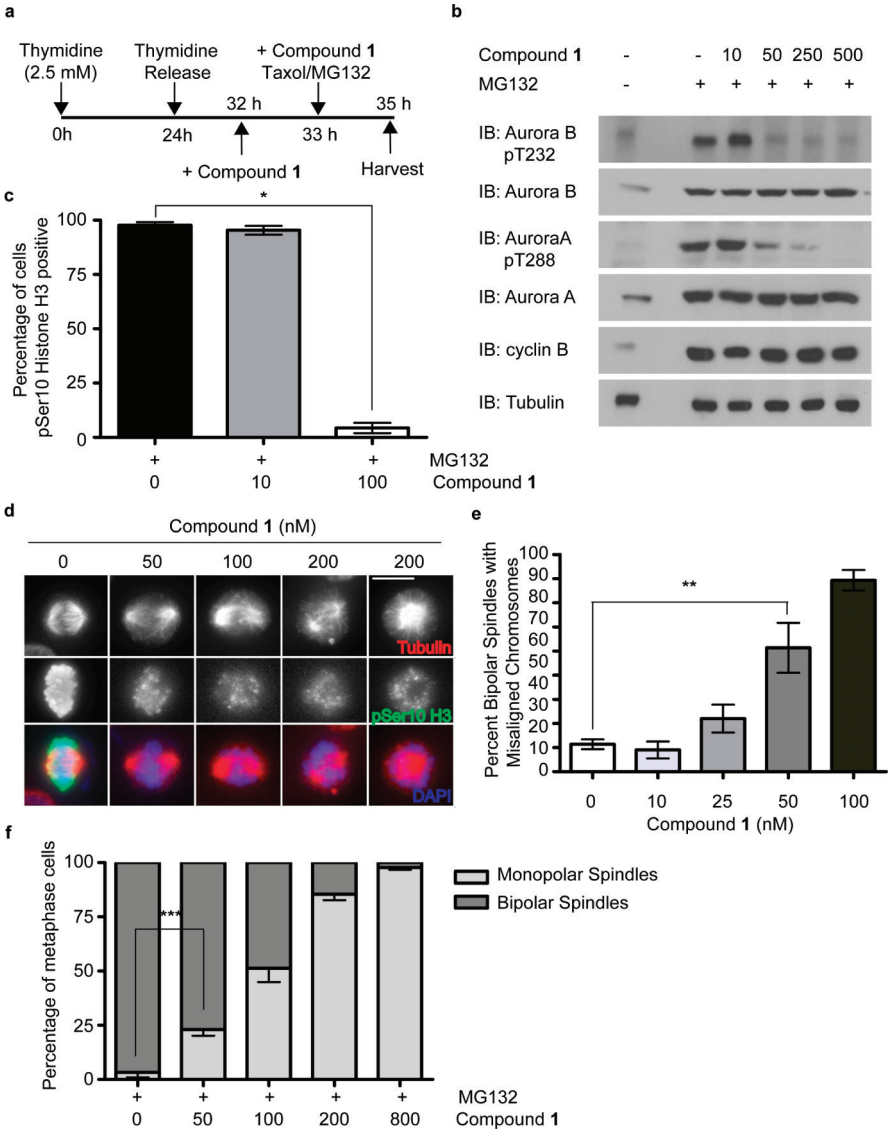

Figure 5. Compound **1** inhibits intracellular functions of Aurora A and B. (a) Schematic of the treatment regimen used to assess the effect of **1** on intracellular Aurora A and B kinase autophosphorylation. (b) Effect of compound **1** on Aurora A and B autophosphorylation. (c) Effect of **1** on the phosphorylation status of Histone H3 Ser10. Cells were fixed and probed for phospho-Ser10 Histone H3. Percentage of cells positive for phospho-Ser10 was determined. *p-value = 8.49×10^{-6}; 300 cells of each cell population were counted. (d) Representative images of cells treated as described in panel c: phospho-Ser10 Histone H3 (green), α-tubulin (red), and DNA (blue). Scale bar represents 10 μm. (e) Effect of **1** treatment on chromosome alignment. The percentage of cells with bipolar spindles exhibiting misaligned chromosomes was determined. **p-value = 1.92×10^{-2}. (f) Effect of **1** treatment on the formation of monopolar spindles. The percentage of cells exhibiting monopolar spindles was determined. ***p-value 6.09×10^{-3}; 300 cells of each cell population were counted.

Aurora B are distinct residues (Thr217 and Glu177, respectively), suggesting that this position of the Aurora kinase scaffold acts as a selectivity filter in binding to these derivatives (Supplementary Figure S2b).

The SAR exploration of the benzo[*e*]pyrimido[5,4-*b*][1,4]-diazepin-6(11*H*)-one scaffold revealed that no substitution at the 2-position of the 2-amino moiety, the combination of 3-trifluoromethyl and 4-(4-ethyl-piperazin-1-yl)-methyl substituents of the 2-amino moiety, *N*-methyl substitution at the lactam position, linkage group (X) of the *N*-methyl substituent, and 3-fluoro substituted anthranilic acid were key structure determinants to achieve potent *in vitro* activity and selectivity of Aurora A *vs* B. The most selective compound, **29**, inhibited Aurora A with an *in vitro* IC_{50} of 13.4 nM and exhibited 36-fold selectivity of Aurora A *vs* B. Despite showing superior *in vitro* selectivity against Aurora B, these trifluoromethyl-functionalized compounds suffered from decreased intracellular selectivity and potency (Supplementary Figures S3−S5). The reason for this discrepancy is not immediately apparent but does not appear to be due to poor cell penetration as demonstrated below.

***In Vitro* Selectivity of Compound 1.** To comprehensively investigate the selectivity of this new class of Aurora inhibitors compounds, **1**, **23**, and **29** were profiled at a concentration of 1 μM using the KINOME*scan* methodology across a panel of 442 kinases.[43] This analysis revealed that these new Aurora inhibitors possessed highly selective profiles with KINOME*scan* selectivity score S_{10} of 0.09, 0.1, and 0.04 for compound **1**, **23**, and **29**, respectively (Supplementary Table S2). This broad spectrum approach offers excellent coverage of

dx.doi.org/10.1021/cb200305u | *ACS Chem. Biol.* 2012, 7, 185−196

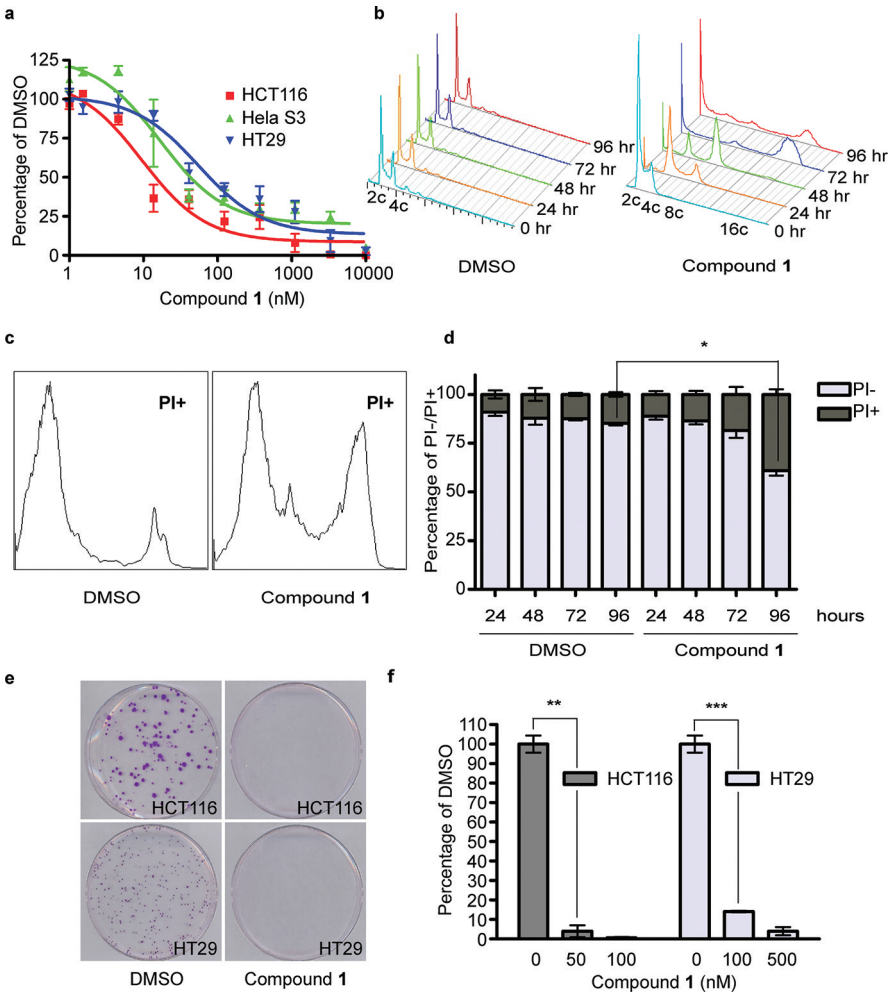

Figure 6. Antiproliferative effect of compound **1**. (a) Effect of compound **1** on the proliferation of HCT116, Hela S3, and HT29 cells following 96 h of treatment. Five independent runs were performed for HCT116/HT29, and 3 independent runs for Hela S3. (b) FACS analysis of HT29 cells treated with DMSO or **1** (500 nM) over the course of 96 h. (c) Effect of compound **1** (500 nM) on cell viability of HT29 cells as judged by propidium iodide (PI) cell viability assay. (d) Quantitation of experiment described in panel c. *p-value = 9.92×10^{-4}. (e) The effect of 50 nM and 100 nM **1** on colony formation of HCT116 and HT29 cells, respectively. (f) Quantitation of experiment described in panel d. **p-value = 5.71×10^{-5}; ***p-value = 4.11×10^{-5}.

the kinome and helped identify a number of potential off-target kinases (Supplementary Table S2). Confirmatory dose–response analysis in biochemical kinase assays for compound **1** revealed sub-100 nM IC_{50} against DCAMKL2, LRRK2, NUAK1, and TAOK1 (Supplementary Table S3). A second complementary chemical proteomics approach using a desthiobiotin-ATP reagent as an ATP-site directed covalent probe was used to study the selectivity of **1** in the context of Hela cell lysates.[44] In this assay format a compound is tested for its ability to protect labeling of the catalytic and/or activation loop lysine by the desthiobiotin-ATP probe (Supplementary Table S4). At 100 nM and 1 μM, concentrations at which the SAC silencing phenotype is fully penetrant, compound **1** displays good selectivity for Aurora kinases. These unbiased approaches demonstrate that up to concentration of 1 μM compound **1** is highly specific inhibitor for Aurora A, B, and C; however, further analysis is required to investigate whether the additional targets mentioned above are indeed bona fide targets at higher concentrations in cells. Compound **1** is a potent biochemical inhibitor of LRRK2 (IC_{50} = 30.5 nM), and this should be considered if it is being employed in scenarios where LRRK2 is expressed.

Compound 1 Inhibits Aurora-Dependent Spindle Assembly Processes. To further characterize whether the cellular effects of **1** were derived from direct inhibition of Aurora kinases, we performed a battery of cellular assays that report on intracellular Aurora activity, which we compared directly with established Aurora inhibitors. Both Aurora A and B demonstrate increase in kinase activity during mitosis as a result of association with accessory proteins that generate fully competent kinase complexes[7−19] and by autophosphorylation of critical residues (T288 AurA and T232 AurB) in the kinase activation (T) loop.[7−9,12,26,45] To assess the effect of **1** on the autophosphorylation status of Aurora A and B, Hela S3 cells were synchronized in mitosis in the presence of DMSO or **1** (Figure 5a). DMSO-treated cells displayed strong Aurora kinase activity, while introduction of **1** led to a dose-dependent decrease in kinase activity with complete inhibition of both Aurora A and B by 250 nM (Figure 5b). Stable cyclin B levels demonstrate that loss of kinase activity was not caused by mitotic exit. Comparison of **1** with **32**, a pan-Aurora kinase inhibitor, revealed similar activities against the activation of Aurora A and B, whereas **33**, an Aurora B-selective agent, displayed moderate intracellular activity against Aurora A

dx.doi.org/10.1021/cb200305u | *ACS Chem. Biol.* 2012, 7, 185–196

Table 3. Enzymatic and Anti-proliferative Activities for Selected Benzo[*e*]pyrimido[5,4-*b*][1,4]diazepin-6(11*H*)-ones and Known Aurora Inhibitors

	1	3	23	29	32	33	34	35
				Enzyme IC_{50} (nM)[a]				
Aur A	5.6	7.2	16.8	13.4	5.6	193	3.0	3.2
Aur B	18.4	25.9	194	487	19.8	15.5	23.2	1380
Aur C	24.6	40.5	419	595	18.3	25.3	9.1	432
				Cell EC_{50} (nM)[b]				
HCT116	9.5	19	553	449	15.8	17.4	50.3	377.6
HT29	55	68	951	1577	118.8	239.2	687.8	5600
HeLa	16.7	10.9	1300	792	16.4	3.8	214	416

[a]The required concentration to inhibit 50% of enzyme activity. [b]The required concentration for inhibiting cell growth at 50%.

(Supplementary Figure S3). All three compounds resulted in a decrease of Ser10 phosphorylation on Histone H3, a known Aurora B substrate (Figure 5c, 5d, and Supplementary Figure S4). Consistent with the known dependence of MT-kinetochore error correction on Aurora B kinase activity, treatment with compound **1** prevented the destabilization of improper connections manifesting significant chromosome congression defects in metaphase cells (Figure 5e and Supplementary Figure S5).

Aurora A localized at the centrosome is responsible for maturation and separation of centrosomes.[32,46−49] Decreased Aurora A kinase activity leads to shortened bipolar spindles as a result of the inability to generate the force necessary to separate centrosomes.[20−22,32] Complete inhibition of Aurora A results in the formation of monopolar spindles. To determine if **1** elicits spindle phenotypes consistent with inhibition of Aurora A, we examined spindle morphology in the presence of **1**. To do so, cells were arrested in metaphase in the presence of DMSO or **1** and the spindle morphology was analyzed by indirect immunofluorescence. Cells treated with **1** exhibited a dose-dependent increase in the frequency of shortened and monopolar spindles with visually complete monopolarity at roughly 800 nM (Figure 5d,f). Similar results were found with **32**, whereas the Aurora B selective **33** did not result in significant monopolarity up to a concentration of 500 nM (Supplementary Figure S5). Together these results indicate that **1** inhibits both Aurora A and B in cells at roughly similar concentrations.

Anti-proliferative Activity. To evaluate the anti-proliferative activity of these new Aurora inhibitors, select compounds were assayed in dose−response format against the human colorectal cancer cell lines HCT116 and HT29 and the human cervical cancer cell line HeLa S3 (Figure 6a, Supplementary Figure S6; Tables 1 and 2). The results suggested that the anti-proliferative activity of a compound correlated closely with its ability to inhibit Aurora B kinase activity. Indeed, the pan-Aurora inhibitors exemplified by **1** and **3** clustered closely with **32** and **33** based on common anti-Aurora B activity, while the Aurora A selective compounds **23** and **29** clustered with the Aurora A selective inhibitors **34** and **35** (Supplementary Figure S6, Tables 1−3). These results are consistent with previous reports demonstrating that the anti-proliferative activity of an Aurora inhibitor appears to correlate with its ability to inhibit Aurora B.[38]

FACS analysis allowed us to follow the relative genomic integrity of cells as they progressed through the time course of the anti-proliferative assay. Congruent with the essential roles of Aurora A and B in the faithful execution of cytokinesis, treatment with **1** caused cells to fail cytokinesis and become polyploid (Figure 6b). Over the course of 96 h cell size increased, cells underwent endoreduplication, and reached DNA contents of 16c. As cells continued to undergo errant rounds of cell division in the presence of **1**, a sub-G1 population, typically indicative of cell death/debris, began to form starting at 48 h. Propidium iodide (PI) staining to differentiate live *vs* dead cells indicated that 72−96 h following treatment with **1** significant cell death was observed in the population (Figure 6c,d). Loss of cell viability was also reflected in an inability of **1**-treated cells to form viable progeny in a colony formation assay (Figure 6e,f). Similar levels of ploidy and cell death were witnessed with comparable concentrations of **32** and **33** (Supplementary Figures S7 and S8).

Despite showing superior *in vitro* selectivity for Aurora A, **23** and **29** suffered from decreased intracellular potency (Supplementary Figures S3−S8). For example, whereas compound **29** inhibited Aurora A with a biochemical IC_{50} of 13.4 nM, significant intracellular Aurora A inhibition was not seen until approximately 500 nM to 1 μM (Supplementary Figures S3−S5). One plausible explanation for this discrepancy is poor cell penetrability. To test this hypothesis we used a two-pronged approach utilizing modified versions of the desthiobiotin-ATP proteomics assay, which allowed us to identify compounds with poor cell penetrability. In brief, cells were pretreated with test compounds or DMSO and lysed, and the lysate was probed with desthiobiotin-ATP reagent. As **23** and **29** exhibit strong activity against Aurora A *in vitro*, it would be expected that these compounds when treated to live cells would remain bound to Aurora A in the lysate and compete with desthiobiotin-ATP for the Aurora A active site. Second, to assess whether these compounds can indeed compete directly for Aurora A, in the absence of intact cellular membrane, lysates were cotreated with **23** (or **29**) and desthiobiotin-ATP. Compounds that can compete with desthiobiotin-ATP directly in lysates but not when pretreated to intact cells are deemed to have poor cell penetrability. Compound **1**, which has demonstrated intracellular activities on Aurora A consistent with its enzyme IC_{50}, served as a positive control. It displayed significant competition against the desthiobiotin-ATP reagent for Aurora A in both lysates and live cell treatment in a dose-dependent manner (Supplementary Figure S9). Despite a diminished dose dependency, compounds **23** and **29** demonstrated comparable ability to compete with the desthiobiotin-ATP probe in the context of lysate and live cell treatment. Therefore, this result cannot support the assertion that poor cell penetrability is the cause of the reduced penetrance of Aurora A-associated phenotypes.

Significance. These studies demonstrate that it is possible to obtain highly potent and selective inhibitors of Aurora

dx.doi.org/10.1021/cb200305u|*ACS Chem. Biol.* 2012, 7, 185−196

kinases directly from a phenotypic cellular screen. Compounds **1** and **3** represent a novel class of pan-Aurora inhibitors with the ability to fully inhibit intracellular Aurora A and B activity at 500 nM concentrations. The phenotypic consequences of treatment of cells with **1** and **3** include cytokinesis failure, endoreduplication, and eventual loss of cell viability consistent with cellular effects established with the pan-Aurora inhibitor **32** and the Aurora B-selective **33**. Previous reports demonstrated that inhibition of Aurora B is the primary source of the anti-proliferative effects elicited by Aurora inhibitors.[38] The results obtained here are consistent with those reports with **1** and **3** clustering with inhibitors displaying strong anti-Aurora B activity in anti-proliferative assays. When co-treated with Taxol, cells exhibited a decrease in Taxol-induced cell death supporting the notion that mitotic arrest is crucial to facilitating Taxol toxicity.

The structures described here resulted from the synthetic evolution of predecessor compounds displaying activities against distinct kinases including Plk1, Mps1, Erk5, and LRRK2.[39−42] These compounds serve as prime examples of how a pyrimidine-based core scaffold can be diversified by ring addition and expansion to generate compounds with differential activities. Subtle modifications to these existing compounds, guided by activity-based profiling, have culminated in potent pan-Aurora inhibitors and Aurora A-selective agents. A co-crystal structure of **1** with *X. laevis* Aurora B illustrated the structural basis for the binding affinity of compound **1**, revealing that it binds in a puckered conformation in the ATP binding site. This co-crystal structure provided a platform for systematic modification of the scaffold to investigate selectivity with respect to other kinases. In addition to selectivity determinants, this SAR study enumerated many structural features that are critical for anti-Aurora activity. Furthermore, an extensive structure−activity relationship study, guided by this structural information, resulted in the identification of compounds with 12- and 36-fold biochemical selectivity for Aurora A that possessed poor cellular activity. The poor cellular activity of the Aurora A-selective inhibitors **23** and **29** does not appear to be a result of poor cell penetration. The weak Aurora A-dependent phenotypes could come as a consequence of the need for a more complete inhibition of Aurora A activity in order to elicit an Aurora A-dependent phenotype relative to the amount of inhibition of Aurora B required for an Aurora B-dependent phenotype. However, the strong Aurora A-dependent phenotypes elicited by the pan-Aurora inhibitors **1** and **3** do not support this explanation.

Compounds from this scaffold class have demonstrated a high degree of selectivity for Aurora kinases. The comparison of these new compounds with currently available inhibitors each with different off-target profiles will further the investigation into the therapeutic value of inhibiting this family of kinases. Furthermore, continued chemical interrogation of this privileged scaffold has potential to further our understanding of its SAR and to identify new kinase targets. Compounds of this scaffold class have shown favorable pharmacokinetic properties,[40] suggesting that these compounds may facilitate inhibition of kinases at physiologically and therapeutically relevant concentrations.

METHODS

Chemistry. Compounds were synthesized by modification of existing procedures (WO/2010/080712). See online Supporting Information for characterization data.

Cell Culture. Hela, Hela S3, and MCF7 cells were grown in Dulbecco's Modified Eagle's Medium (DMEM, Sigma), and HCT116 and HT29 cells were grown in McCoy's 5A (Invitrogen). All cell lines were supplemented with 10% FBS (Sigma) and 100 U mL^{-1} penicillin and 100 $\mu g \cdot mL^{-1}$ streptomycin (Invitrogen) and cultured at 37 °C in a humidified chamber in the presence of 5% CO_2, unless otherwise noted.

***In Vitro* Kinase Assay (Mitotic Kinase Panel).** The conditions for the kinase assays shown in Figure 3a have been previously described.[29]

Immunofluorescence. Protocols for immunofluorescence have been previously described.[41]

Mitotic Checkpoint Assays. Hela S3 were plated at roughly 40% cell density. The following day the cells were treated with medium containing thymidine for 24 h. After thymidine block, the cells were washed with PBS and replaced with fresh medium for 8 h, after which time medium containing test compound was added for 1 h followed by co-treatment with test compound and Taxol. After 4 h, the cells were harvested, and the mitotic index was determined by immunoblotting for cyclin B. For experiments examining phosphorylation of Aurora A and B, cells were treated as above but were co-treated with Taxol and MG132 for 2 h prior to harvesting and immunoblotting.

Fluorescence-Activated Cell Sorting Analysis (FACS). Cells were treated with compound for various periods of time. Cells were trypsinized, washed once in phosphate-buffered saline (PBS), and fixed overnight at −20 °C with 80% ethanol in PBS. Cells were washed three times with PBS. Finally, cells were resuspended in PBS containing 0.1% Triton X-100, 25 μg mL^{-1} propidium iodide (PI, Molecular Probes), and 0.2 mg mL^{-1} RNase A (Sigma) and incubated for 45 min at 37 °C. For discrimination of live and dead cells by PI staining, cells were treated with compound for various periods of time. Cells were trypsinized, washed with PBS, and treated with PBS containing 25 μg mL^{-1} PI. Cell cycle distribution or PI stain for viability was determined on a BD FACScan (BD Biosciences) and analyzed on FlowJo (Treestar).

Proliferation, Colony Outgrowth. Taxol sensitivity proliferation assays and colony formation assays were performed as previously described,[40,41] Proliferation assays testing compounds alone were conducted using Cell Titer Glo as described in product manual.

ASSOCIATED CONTENT

Supporting Information

This material is available free of charge via the Internet at http://pubs.acs.org.

Accession Codes

X-ray coordinates and structure factors have been deposited in the Protein Data Bank. PDB accession code: 3ZTX.

AUTHOR INFORMATION

Corresponding Author

*E-mail: nathanael_gray@dfci.harvard.edu.

Present Address

[¶]Koch Institute for Integrative Cancer Research, Massachusetts Institute of Technology, Cambridge, MA 02139.

Author Contributions

[#]These authors contributed equally to this work.

Notes

The authors declare no competing financial interests.

ACKNOWLEDGMENTS

We thank DiscoveRx (Ambit Biosciences) for performing KINOME*scan*, Life Technologies Corporation for performing SelectScreen Kinase Profiling and ActivX for performing KiNativ analysis, as well as the Nikon Imaging Facility (HMS) and the Dana Farber Flow Cytometry Lab (DFCI)

for technical help and instrument use. Funding was provided by NIH grants CA130876-03, HG005693-02, U54 HG006097-01. The HMS LINCS Center is funded by NIH U54 HG006097, and NIH Grand Opportunities grant 1RC2HG005693. A.M. acknowledges generous funding from the Italian Association for Cancer Research. S.S. is supported by a fellowship from the Italian Foundation for Cancer Research.

REFERENCES

(1) Huang, H. C., Shi, J., Orth, J. D., and Mitchison, T. J. (2009) Evidence that mitotic exit is a better cancer therapeutic target than spindle assembly. *Cancer Cell 16*, 347−358.

(2) Rieder, C. L., and Maiato, H. (2004) Stuck in division or passing through: What happens when cells cannot satisfy the spindle assembly checkpoint. *Dev. Cell 7*, 637−651.

(3) Shi, J., Orth, J. D., and Mitchison, T. (2008) Cell type variation in responses to antimitotic drugs that target microtubules and kinesin-5. *Cancer Res. 68*, 3269−3276.

(4) George, J., Banik, N. L., and Ray, S. K. (2009) Combination of taxol and Bcl-2 siRNA induces apoptosis in human glioblastoma cells and inhibits invasion, angiogenesis and tumour growth. *J. Cell. Mol. Med. 13*, 4205−4218.

(5) Tan, N., Malek, M., Zha, J., Yue, P., Kassees, R., Berry, L., Fairbrother, W. J., Sampath, D., and Belmont, L. D. (2011) Navitoclax enhances the efficacy of taxanes in non-small cell lung cancer models. *Clin. Cancer Res. 17*, 1394−1404.

(6) Wertz, I. E., Kusam, S., Lam, C., Okamoto, T., Sandoval, W., Anderson, D. J., Helgason, E., Ernst, J. A., Eby, M., Liu, J., Belmont, L. D., Kaminker, J. S., O'Rourke, K. M., Pujara, K., Kohli, P. B., Johnson, A. R., Chiu, M. L., Lill, J. R., Jackson, P. K., Fairbrother, W. J., Seshagiri, S., Ludlam, M. J., Leong, K. G., Dueber, E. C., Maecker, H., Huang, D. C., and Dixit, V. M. (2011) Sensitivity to antitubulin chemotherapeutics is regulated by MCL1 and FBW7. *Nature 471*, 110−114.

(7) Bayliss, R., Sardon, T., Vernos, I., and Conti, E. (2003) Structural basis of Aurora-A activation by TPX2 at the mitotic spindle. *Mol. Cell 12*, 851−862.

(8) Bishop, J. D., and Schumacher, J. M. (2002) Phosphorylation of the carboxyl terminus of inner centromere protein (INCENP) by the Aurora B kinase stimulates Aurora B kinase activity. *J. Biol. Chem. 277*, 27577−27580.

(9) Bolton, M. A., Lan, W., Powers, S. E., McCleland, M. L., Kuang, J., and Stukenberg, P. T. (2002) Aurora B kinase exists in a complex with survivin and INCENP and its kinase activity is stimulated by survivin binding and phosphorylation. *Mol. Biol. Cell 13*, 3064−3077.

(10) Chen, J., Jin, S., Tahir, S. K., Zhang, H., Liu, X., Sarthy, A. V., McGonigal, T. P., Liu, Z., Rosenberg, S. H., and Ng, S. C. (2003) Survivin enhances Aurora-B kinase activity and localizes Aurora-B in human cells. *J. Biol. Chem. 278*, 486−490.

(11) Eyers, P. A., Erikson, E., Chen, L. G., and Maller, J. L. (2003) A novel mechanism for activation of the protein kinase Aurora A. *Curr. Biol. 13*, 691−697.

(12) Honda, R., Korner, R., and Nigg, E. A. (2003) Exploring the functional interactions between Aurora B, INCENP, and survivin in mitosis. *Mol. Biol. Cell 14*, 3325−3341.

(13) Hutterer, A., Berdnik, D., Wirtz-Peitz, F., Zigman, M., Schleiffer, A., and Knoblich, J. A. (2006) Mitotic activation of the kinase Aurora-A requires its binding partner Bora. *Dev. Cell 11*, 147−157.

(14) Jelluma, N., Brenkman, A. B., van den Broek, N. J., Cruijsen, C. W., van Osch, M. H., Lens, S. M., Medema, R. H., and Kops, G. J. (2008) Mps1 phosphorylates Borealin to control Aurora B activity and chromosome alignment. *Cell 132*, 233−246.

(15) Jeyaprakash, A. A., Klein, U. R., Lindner, D., Ebert, J., Nigg, E. A., and Conti, E. (2007) Structure of a Survivin-Borealin-INCENP core complex reveals how chromosomal passengers travel together. *Cell 131*, 271−285.

(16) Kelly, A. E., Sampath, S. C., Maniar, T. A., Woo, E. M., Chait, B. T., and Funabiki, H. (2007) Chromosomal enrichment and activation of the aurora B pathway are coupled to spatially regulate spindle assembly. *Dev. Cell 12*, 31−43.

(17) Kufer, T. A., Sillje, H. H., Korner, R., Gruss, O. J., Meraldi, P., and Nigg, E. A. (2002) Human TPX2 is required for targeting Aurora-A kinase to the spindle. *J. Cell Biol. 158*, 617−623.

(18) Sessa, F., Mapelli, M., Ciferri, C., Tarricone, C., Areces, L. B., Schneider, T. R., Stukenberg, P. T., and Musacchio, A. (2005) Mechanism of Aurora B activation by INCENP and inhibition by hesperadin. *Mol. Cell 18*, 379−391.

(19) Vader, G., Kauw, J. J., Medema, R. H., and Lens, S. M. (2006) Survivin mediates targeting of the chromosomal passenger complex to the centromere and midbody. *EMBO Rep. 7*, 85−92.

(20) Glover, D. M., Leibowitz, M. H., McLean, D. A., and Parry, H. (1995) Mutations in aurora prevent centrosome separation leading to the formation of monopolar spindles. *Cell 81*, 95−105.

(21) Hirota, T., Kunitoku, N., Sasayama, T., Marumoto, T., Zhang, D., Nitta, M., Hatakeyama, K., and Saya, H. (2003) Aurora-A and an interacting activator, the LIM protein Ajuba, are required for mitotic commitment in human cells. *Cell 114*, 585−598.

(22) Kimura, M., Kotani, S., Hattori, T., Sumi, N., Yoshioka, T., Todokoro, K., and Okano, Y. (1997) Cell cycle-dependent expression and spindle pole localization of a novel human protein kinase, Aik, related to Aurora of Drosophila and yeast Ipl1. *J. Biol. Chem. 272*, 13766−13771.

(23) Bird, A. W., and Hyman, A. A. (2008) Building a spindle of the correct length in human cells requires the interaction between TPX2 and Aurora A. *J. Cell Biol. 182*, 289−300.

(24) Koffa, M. D., Casanova, C. M., Santarella, R., Kocher, T., Wilm, M., and Mattaj, I. W. (2006) HURP is part of a Ran-dependent complex involved in spindle formation. *Curr. Biol. 16*, 743−754.

(25) Tsai, M. Y., Wiese, C., Cao, K., Martin, O., Donovan, P., Ruderman, J., Prigent, C., and Zheng, Y. (2003) A Ran signalling pathway mediated by the mitotic kinase Aurora A in spindle assembly. *Nat. Cell Biol. 5*, 242−248.

(26) Cheeseman, I. M., Anderson, S., Jwa, M., Green, E. M., Kang, J., Yates, J. R. 3rd, Chan, C. S., Drubin, D. G., and Barnes, G. (2002) Phospho-regulation of kinetochore-microtubule attachments by the Aurora kinase Ipl1p. *Cell 111*, 163−172.

(27) Lampson, M. A., Renduchitala, K., Khodjakov, A., and Kapoor, T. M. (2004) Correcting improper chromosome-spindle attachments during cell division. *Nat. Cell Biol. 6*, 232−237.

(28) Tanaka, T. U., Rachidi, N., Janke, C., Pereira, G., Galova, M., Schiebel, E., Stark, M. J., and Nasmyth, K. (2002) Evidence that the Ipl1-Sli15 (Aurora kinase-INCENP) complex promotes chromosome bi-orientation by altering kinetochore-spindle pole connections. *Cell 108*, 317−329.

(29) Santaguida, S., Tighe, A., D'Alise, A. M., Taylor, S. S., and Musacchio, A. (2010) Dissecting the role of MPS1 in chromosome biorientation and the spindle checkpoint through the small molecule inhibitor reversine. *J. Cell Biol. 190*, 73−87.

(30) Santaguida, S., Vernieri, C., Villa, F., Ciliberto, A., and Musacchio, A. (2011) Evidence that Aurora B is implicated in spindle checkpoint signalling independently of error correction. *EMBO J. 30*, 1508−1519.

(31) Saurin, A. T., van der Waal, M. S., Medema, R. H., Lens, S. M., and Kops, G. J. (2011) Aurora B potentiates Mps1 activation to ensure rapid checkpoint establishment at the onset of mitosis. *Nat. Commun. 2*, 316.

(32) Giet, R., McLean, D., Descamps, S., Lee, M. J., Raff, J. W., Prigent, C., and Glover, D. M. (2002) Drosophila Aurora A kinase is required to localize D-TACC to centrosomes and to regulate astral microtubules. *J. Cell Biol. 156*, 437−451.

(33) Terada, Y., Tatsuka, M., Suzuki, F., Yasuda, Y., Fujita, S., and Otsu, M. (1998) AIM-1: a mammalian midbody-associated protein required for cytokinesis. *EMBO J. 17*, 667−676.

(34) Aliagas-Martin, I., Burdick, D., Corson, L., Dotson, J., Drummond, J., Fields, C., Huang, O. W., Hunsaker, T., Kleinheinz, T., Krueger, E., Liang, J., Moffat, J., Phillips, G., Pulk, R., Rawson, T. E., Ultsch, M., Walker, L., Wiesmann, C., Zhang, B., Zhu, B. Y., and

Cochran, A. G. (2009) A class of 2,4-bisanilinopyrimidine Aurora A inhibitors with unusually high selectivity against Aurora B. *J. Med. Chem. 52*, 3300−3307.

(35) Harrington, E. A., Bebbington, D., Moore, J., Rasmussen, R. K., Ajose-Adeogun, A. O., Nakayama, T., Graham, J. A., Demur, C., Hercend, T., Diu-Hercend, A., Su, M., Golec, J. M., and Miller, K. M. (2004) VX-680, a potent and selective small-molecule inhibitor of the Aurora kinases, suppresses tumor growth *in vivo*. *Nat. Med. 10*, 262−267.

(36) Manfredi, M. G., Ecsedy, J. A., Meetze, K. A., Balani, S. K., Burenkova, O., Chen, W., Galvin, K. M., Hoar, K. M., Huck, J. J., LeRoy, P. J., Ray, E. T., Sells, T. B., Stringer, B., Stroud, S. G., Vos, T. J., Weatherhead, G. S., Wysong, D. R., Zhang, M., Bolen, J. B., and Claiborne, C. F. (2007) Antitumor activity of MLN8054, an orally active small-molecule inhibitor of Aurora A kinase. *Proc. Natl. Acad. Sci. U.S.A. 104*, 4106−4111.

(37) Mortlock, A. A., Foote, K. M., Heron, N. M., Jung, F. H., Pasquet, G., Lohmann, J. J., Warin, N., Renaud, F., De Savi, C., Roberts, N. J., Johnson, T., Dousson, C. B., Hill, G. B., Perkins, D., Hatter, G., Wilkinson, R. W., Wedge, S. R., Heaton, S. P., Odedra, R., Keen, N. J., Crafter, C., Brown, E., Thompson, K., Brightwell, S., Khatri, L., Brady, M. C., Kearney, S., McKillop, D., Rhead, S., Parry, T., and Green, S. (2007) Discovery, synthesis, and *in vivo* activity of a new class of pyrazoloquinazolines as selective inhibitors of aurora B kinase. *J. Med. Chem. 50*, 2213−2224.

(38) Girdler, F., Sessa, F., Patercoli, S., Villa, F., Musacchio, A., and Taylor, S. (2008) Molecular basis of drug resistance in aurora kinases. *Chem. Biol. 15*, 552−562.

(39) Deng, X., Dzamko, N., Prescott, A., Davies, P., Liu, Q., Yang, Q., Lee, J. D., Patricelli, M. P., Nomanbhoy, T. K., Alessi, D. R., and Gray, N. S. (2011) Characterization of a selective inhibitor of the Parkinson's disease kinase LRRK2. *Nat. Chem. Biol. 7*, 203−205.

(40) Deng, X., Yang, Q., Kwiatkowski, N., Sim, T., McDermott, U., Settleman, J. E., Lee, J. D., and Gray, N. S. (2011) Discovery of a benzo[*e*]pyrimido-[5,4-*b*][1,4]diazepin-6(11*H*)-one as a potent and selective inhibitor of big MAP Kinase 1. *ACS Med. Chem. Lett. 2*, 195−200.

(41) Kwiatkowski, N., Jelluma, N., Filippakopoulos, P., Soundararajan, M., Manak, M. S., Kwon, M., Choi, H. G., Sim, T., Deveraux, Q. L., Rottmann, S., Pellman, D., Shah, J. V., Kops, G. J., Knapp, S., and Gray, N. S. (2010) Small-molecule kinase inhibitors provide insight into Mps1 cell cycle function. *Nat. Chem. Biol. 6*, 359−368.

(42) Lenart, P., Petronczki, M., Steegmaier, M., Di Fiore, B., Lipp, J. J., Hoffmann, M., Rettig, W. J., Kraut, N., and Peters, J. M. (2007) The small-molecule inhibitor BI 2536 reveals novel insights into mitotic roles of polo-like kinase 1. *Curr. Biol. 17*, 304−315.

(43) Fabian, M. A., Biggs, W. H. 3rd, Treiber, D. K., Atteridge, C. E., Azimioara, M. D., Benedetti, M. G., Carter, T. A., Ciceri, P., Edeen, P. T., Floyd, M., Ford, J. M., Galvin, M., Gerlach, J. L., Grotzfeld, R. M., Herrgard, S., Insko, D. E., Insko, M. A., Lai, A. G., Lelias, J. M., Mehta, S. A., Milanov, Z. V., Velasco, A. M., Wodicka, L. M., Patel, H. K., Zarrinkar, P. P., and Lockhart, D. J. (2005) A small molecule-kinase interaction map for clinical kinase inhibitors. *Nat. Biotechnol. 23*, 329−336.

(44) Patricelli, M. P., Szardenings, A. K., Liyanage, M., Nomanbhoy, T. K., Wu, M., Weissig, H., Aban, A., Chun, D., Tanner, S., and Kozarich, J. W. (2007) Functional interrogation of the kinome using nucleotide acyl phosphates. *Biochemistry 46*, 350−358.

(45) Yasui, Y., Urano, T., Kawajiri, A., Nagata, K., Tatsuka, M., Saya, H., Furukawa, K., Takahashi, T., Izawa, I., and Inagaki, M. (2004) Autophosphorylation of a newly identified site of Aurora-B is indispensable for cytokinesis. *J. Biol. Chem. 279*, 12997−13003.

(46) Abe, Y., Ohsugi, M., Haraguchi, K., Fujimoto, J., and Yamamoto, T. (2006) LATS2-Ajuba complex regulates gamma-tubulin recruitment to centrosomes and spindle organization during mitosis. *FEBS Lett. 580*, 782−788.

(47) Hannak, E., Kirkham, M., Hyman, A. A., and Oegema, K. (2001) Aurora-A kinase is required for centrosome maturation in Caenorhabditis elegans. *J. Cell Biol. 155*, 1109−1116.

(48) Mori, D., Yano, Y., Toyo-oka, K., Yoshida, N., Yamada, M., Muramatsu, M., Zhang, D., Saya, H., Toyoshima, Y. Y., Kinoshita, K., Wynshaw-Boris, A., and Hirotsune, S. (2007) NDEL1 phosphorylation by Aurora-A kinase is essential for centrosomal maturation, separation, and TACC3 recruitment. *Mol. Cell. Biol. 27*, 352−367.

(49) Toji, S., Yabuta, N., Hosomi, T., Nishihara, S., Kobayashi, T., Suzuki, S., Tamai, K., and Nojima, H. (2004) The centrosomal protein Lats2 is a phosphorylation target of Aurora-A kinase. *Genes Cells 9*, 383−397.